Available online at www.sciencedirect.com
ScienceDirect
Chinese Journal of Natural Medicines 2021, **19**(3): 195-204
doi: 10.1016/S1875-5364(21)60021-3
Chinese Journal of Natural Medicines

•Research article•

Paris saponin VII, a direct activator of AMPK, induces autophagy and exhibits therapeutic potential in non-small-cell lung cancer

XIANG Yu-Chen[1, 2Δ], SHEN Jie[1, 2Δ], SI Yuan[1, 2, 3], LIU Xue-Wen[2, 3], ZHANG Liang[1, 2], WEN Jun[1, 2], ZHANG Te[2, 4], YU Qing-Qing[2, 4], LU Jun-Fei[1, 2], XIANG Ke[5], LIU Ying[1, 2, 3, 4*]

[1] *Laboratory of Molecular Target Therapy of Cancer, Institute of Basic Medical Sciences, Hubei University of Medicine, Shiyan 442000, China;*
[2] *Hubei Key Laboratory of Wudang Local Chinese Medicine Research and Institute of Medicinal Chemistry, Hubei University of Medicine, Shiyan 442000, China;*
[3] *Hubei Key Laboratory of Embryonic Stem Cell Research, Hubei University of Medicine, Shiyan 442000, China;*
[4] *Laboratory of Molecular Target Therapy of Cancer, Biomedical Research Institute, Hubei University of Medicine, Shiyan 442000, China;*
[5] *Department of Science and Education, Gucheng People's Hospital, Hubei University of Arts and Science, Xiangyang 441700, China*

Available online 20 Mar., 2021

[ABSTRACT] Paris saponin VII (PSVII), a bioactive constituent extracted from *Trillium tschonoskii* Maxim., is cytotoxic to several cancer types. This study was designed to explore whether PSVII prevents non-small-cell lung cancer (NSCLC) proliferation and to investigate its molecular target. AMP-activated protein kinase (AMPK) has been implicated in the activation of autophagy in distinct tissues. In cultured human NSCLC cell lines, PSVII induces autophagy by activating AMPK and inhibiting mTOR signaling. Furthermore, PSVII-induced autophagy activation was reversed by the AMPK inhibitor compound C. Computational docking analysis showed that PSVII directly interacted with the allosteric drug and metabolite site of AMPK to stabilize its activation. Microscale thermophoresis assay and drug affinity responsive target stability assay further confirmed the high affinity between PSVII and AMPK. In summary, PSVII acts as a direct AMPK activator to induce cell autophagy, which inhibits the growth of NSCLC cells. In the future, PSVII therapy should be applied to treat patients with NSCLC.

[KEY WORDS] Paris saponin VII; NSCLC; Autophagy; AMPK
[CLC Number] R965 **[Document code]** A **[Article ID]** 2095-6975(2021)03-0195-10

Introduction

Lung cancer is one of most common malignant tumors worldwide, and its incidence and mortality are continuing to increase. In 2018, a total of 2 093 876 cases of lung cancer were newly diagnosed, accounting for 11.6% of the total cases and 1 761 007 mortality cases have been estimated worldwide [1]. In addition, the morbidity and mortality rates of this disease rank at the top of different types of tumors in China [2]. Lung cancer mainly includes small-cell lung cancer and non-small-cell lung cancer (NSCLC). NSCLC accounts for approximately 80% of lung cancers. The 5-year survival rate of NSCLC is < 15% [3-4]. The treatments for NSCLC mainly include surgery, chemotherapy, radiotherapy and targeted therapy, depending on the histological type and stage at diagnosis. However, the effects of treatment on patients with late-stage NSCLC are dissatisfactory [5]. Therefore, strategies to explore novel anticancer agents for NSCLC should be a promising way to prolong the survival of late-stage patients.

Autophagy is a protective 'self-eating' metabolic pro-

[Received on] 13-Jul.-2020
[Research funding] This work was supported by the National Natural Science Foundation of China (Nos. 82072928 and 81802387), the Foundation for Innovative Research Team of Hubei Provincial Department of Education (No. T201915), Hubei Provincial Technology Innovation Project (No. 2017ACA176), the Innovative Research Program for Graduates (No. YC2019001), the Principal Investigator Grant of Hubei University of Medicine (No. HBMUPI201806), the Grants of Open Ended Design Project from Hubei Key Laboratory of Wudang Local Chinese Medicine Research (No. WDCM2019008), and the Faculty Development Grants from Hubei University of Medicine (Nos. 2018QDJZR03 and 2019QDJZR16).
[*Corresponding author] E-mail: ying_liu1002@163.com
[Δ]These authors contributed equally to this work.
These authors have no conflict of interest to declare.

cess that is devoted to the lysosomal degradation pathway. In this process, proteins and organelles are first phagocytized by autophagosomes, delivered to lysosomes and finally degraded and recycled [6]. Increasing evidence shows that autophagy is vitally involved not only in basic physiological states but also in the pathology of various human diseases [7]. In fact, some tumors rely on autophagy for survival, and tumor cells can exploit autophagy to respond to the cytotoxicity of certain anticancer drugs. However, certain therapies seem to require autophagy to effectively kill cancer cells [8]. Despite these dichotomies, autophagy clearly plays an important role in cancer [9]. Therefore, targeting the autophagy process is considered as a new therapeutic approach and it could provide new treatments for cancer [10].

Adenosine monophosphate-activated protein kinase (AMPK) is an important energy sensor that regulates cell metabolism and maintains energy homeostasis [11]. In addition, AMPK is a positive regulator of autophagy and a tumor suppressor that regulates autophagy in cancer cells [12-14]. Accordingly, AMPK activators have been identified as potential targeted drugs for the treatment of human cancer, and there is a need to develop novel AMPK activators with a low toxicity and high efficiency for inducing tumor cell autophagic suicide.

Trillium tschonoskii Maxim (TTM) is a pharmacologically important medicinal plant in the trackless wilderness regions of the Wudang Mountains and Shennongjia National Nature Reserve of China that is known locally as *Yan Ling Cao* or "a bead above the head" [15-16]. In folk medicine, the rhizomes of TTM are used to treat hypertension, neurasthenia, headache, irregular menstruation, traumatic bleeding, and various inflammatory diseases [17]. Paris saponin VII (PSVII, Fig. 1), a steroidal saponin isolated from the rhizome of TTM, exhibits preclinical antitumor efficacy in several cancer types, including colorectal cancer, cervical cancer, lung cancer, and osteosarcoma [18-21]. The aim of the present study was to evaluate the antitumor effect and potential molecular target of PSVII in NSCLC.

Materials and Methods

Reagents

PSVII with a purity of up to 95% was purchased from Shanghai YuanYe Bio-Technology Co., Ltd. (Shanghai, China). PSVII was dissolved in dimethylsulfoxide (DMSO, Sigma-Aldrich, Merck KGaA, Darmstadt, Germany) at a stock solution of 50 mmol·L^{-1} and stored at −20 °C. Compound C (BML-275, Dorsomorphin; catalog no. 866405-64-3) was purchased from Sigma-Aldrich.

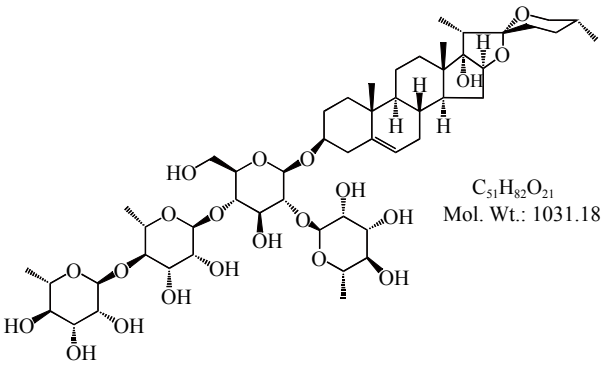

Fig. 1 Structure of PSVII

Cell culture

Human NSCLC cell lines A549, NCI-H820 (H820), PC9, NCI-H460 (H460), H1299, and human normal lung epithelial cell line (16-HBE) were obtained from American Type Culture Collection (ATCC, Manassas, VA, USA). A549, PC9, H460, H1299, and 16-HBE cells were cultured in Dulbecco modified Eagle medium (DMEM, Gibco; Thermo Fisher Scientific, Inc., Waltham, MA, USA). H820 cells were cultured in RPMI 1640 medium (Gibco, Thermo Fisher Scientific, Inc.). DMEM and RPMI 1640 medium were supplemented with 10% fetal bovine serum (FBS, HyClone, Logan, UT, USA), 100 U·mL^{-1} penicillin, and 100 μg·mL^{-1} streptomycin (both from Gibco, Thermo Fisher Scientific, Inc.) and cultured in a humidified atmosphere with 5% CO_2 at 37 °C.

Cytotoxic assay, cell viability

Cells were seeded onto a 96-well plate, pre-cultured for 4 h, and then treated with PSVII for 24 h. Cell cytotoxicity was investigated by a CCK-8 assay. The absorbance was determined at 450 nm by an automated microplate reader (Bio-Tek, VT, USA), and the inhibition rate was calculated as follows: Inhibition rate = (average A_{450} of the control group – average A_{450} of the experimental group)/(average A_{450} of the control group – average A_{450} of the blank group) × 100%. Cell viability was determined by trypan blue dye exclusion.

Soft agar colony formation assay

Cells were suspended in 1 mL of DMEM containing 0.3% low-melting-point agarose (Amresco, Cleveland, Oh, USA) and 10% FBS, and plated on a bottom layer containing 0.6% agarose and 10% FBS in 6-well plate in triplicate. After 2 weeks, plates were stained with 0.2% gentian violet and the colonies were counted under light microscope (IX70, Olympus Corporation, Tokyo, Japan) after 2 weeks.

Flow cytometry assays

Cells were seeded in 6-well plate and incubated with PSVII for 24 h. Cell apoptosis was evaluated by AV/PI detection using an AV-FITC kit (BD Biosciences, San Jose, CA, USA), flow cytometry was performed using a BD FACScanto II flow cytometer (Becton Dickinson, San Jose, CA), and at least 10 000 cells were counted for each sample [22].

DAPI staining

To observe nuclear morphology, cells treated under the indicated conditions were fixed in 4% paraformaldehyde, incubated with 4′,6-diamidino-2-phenylindole (DAPI; Sigma Chemical Co.), and then analyzed using a fluorescence microscope (Olympus, Japan).

Western blot analysis

Cells were harvested and lysed with RIPA buffer to extract total protein. Total protein was loaded on 8% to 12% SDS-PAGE. Subsequently, the gel was electrophoretically

transferred to a PVDF membrane (Millipore, Kenilworth, NJ, USA). After blocking with 5% nonfat dry milk for 1 h at room temperature, the membrane was incubated with the primary antibody overnight at 4 °C and washed three times with Tris buffered saline containing 0.5% Tween-20. The following primary antibodies were used: anti-cleaved caspase-3 (1 ∶ 1000; catalog No. 9664), anti-cleaved caspase-8 (1 ∶ 1000; catalog No. 9748), anti-cleaved PARP (1 ∶ 1000; catalog No. 9548), anti-LC3 (1 ∶ 1000; catalog No. 12741), anti-AMPKα (1 ∶ 1000; catalog No. 2532), anti-phospho-AMPKα (Thr172) (1 ∶ 1000; catalog No. 2535), anti-mTOR (1 ∶ 1000; catalog No. 2983), anti-phospho-mTOR (Ser2448) (1 ∶ 1000; catalog No. 5536), anti-P70S6K (1 ∶ 1000; catalog No. 9202), anti-phospho-P70S6K (Thr389) (1 ∶ 1000; catalog No. 92775), anti-4EBP1 (1 ∶ 1000; catalog No. 9234), anti-phospho-4EBP1 (Thr37/46) (1 ∶ 1000; catalog No. 2855) (Cell Signaling Technology, Inc., Danvers, MA, USA), anti-p62 (1 ∶ 1000; catalog No. P0067; Sigma), and anti-GAPDH (1 ∶ 5000; catalog No. M20006; Abmart, Shanghai, China). The blots were then washed, and incubated with a horseradish peroxidase (HRP)-conjugated secondary antibody (1 ∶ 10 000; catalog No. E030120-01 (rabbit) and E030110-01 (mouse); EarthOx, LLC, San Francisco, CA, USA) at room temperature for 1.5 h. Detection was performed using a SuperSignal® West Pico Trial kit (catalog No. QA210131; Pierce Biotechnology, Inc., Rockford, IL, USA) [23].

Autophagy assays

The cells were transfected with pQCXIP-GFP-LC3 plasmid using the Lipofectamine 3000 (Invitrogen; Thermo Fisher Scientific, Inc.) according to the recommended protocol by the manufacturer and then fixed in 4% paraformaldehyde. The percentage of cells with fluorescent dots representing GFP-LC3 translocation was counted. For visualization of cell nucleus, DAPI was used. Sections were observed using an Olympus laser scanning confocal microscope with imaging software (Olympus Fluoview FV-1000, Tokyo, Japan) [24].

AMPK activity assay

AMPK kinase activity was assay was performed by AMPK kinase activity kit which was purchased from CycLex Co., Ltd. (Cat#CY-1182). Absorbance was measured at 450 nm.

Molecular docking

Ligand docking studies were performed with Autodock 4. The structure of AMPK (PDB code: 4CFF) was obtained from the protein data bank. α is green, β is cyan, γ is magenta and the ligands are brown. The chemical structure of PSVII is shown in Fig. 1. Docking was performed with the docking box sizes large enough to include the binding sites.

Microscale thermophoresis assay

Mixed the different concertation of PSVII with labelled Homo AMPK$\alpha\beta\gamma$ (Abcam, Cambridge, UK) and incubated for 30 min at room temperature. The specimens were loaded and measured on a Monolith NT.115 instrument (Nano Temper Technologies, München, Germany). The dissociation constant (K_d) values were fitted by the NT Analysis software (Nano Temper Technologies, München, Germany) [25].

Drug affinity responsive target stability assay

Cells were harvested and lysed with Cell Lysis Buffer (Thermo Fisher Scientific, Inc., Waltham, MA, USA) to extract total protein. Total protein was treated with different concentration of PSVII and incubated with pronase (Sigma) at 37 °C for 30 min. The extent of hydrolyzation of each specimen was measured by western blot [26].

Statistical analysis

All statistical analyses were conducted using GraphPad Prism 8 (GraphPad Software, Inc., La Jolla, CA, USA) and SPSS 22.0 software for Windows (IBM Corp., Armonk, NY, USA). Results from three independent experiments were presented as the mean ± standard deviation unless otherwise noted. Statistically significant values were compared using Student's *t*-test of unpaired data or one-way analysis of variance and Bonferroni's post hoc test. $P < 0.05$ was used to indicate a statistically significant difference.

Results

PSVII inhibits the proliferation of NSCLC cells

We tested the effects of PSVII on lung cancer and the normal human bronchial epithelial cell line 16-HBE and found that 16-HBE cells has reduced sensitivity to PSVII, with an IC_{50} value of 7.62 μmol·L^{-1}. The IC_{50} values of PSVII against H460 and PC9 cells were 3.16 and 2.86 μmol·L^{-1}, respectively, at 24 h (Figs. 2A–2B, Table 1). Trypan blue exclusion assays showed that PSVII reduced the number of viable H460 (Fig. 2C) and PC9 (Fig. 2D) cells in a dose- and time-dependent manner. We also verified the effect of PSVII on colony formation. The results showed that PSVII markedly inhibited the clonogenic ability of H460 (Fig. 2E) and PC9 (Fig. 2F) cells. These results suggest that PSVII inhibits anchorage-dependent (cell viability) and anchorage-independent (colony formation) growth of NSCLC cells.

PSVII induces the caspase-dependent apoptosis in NSCLC cells

We next investigated whether PSVII activates apoptosis in H460 and PC9 cells. AV/PI-staining and flow cytometry assays confirmed that PSVII treatment activated apoptosis in H460 and PC9 (Fig. 3A) cells. DAPI staining further showed that PSVII induced chromatin condensation and fragmentation in H460 and PC9 cells, which showed typical nuclear morphological changes that are indicative of apoptosis (Fig. 3B). Next, Western blot analysis showed that PSVII induced a significant increase in the cleaved form of caspase-3 (cleaved casp3), and caspase-8 (cleaved casp8) and induced cleavage of poly ADP-ribose polymerase (PARP) in H460 and PC9 cells (Fig. 3C). These results indicate that PSVII activates caspase-dependent apoptosis in NSCLC cells.

PSVII induces autophagosome formation and blocks autophagic flux in NSCLC cells

Autophagy is a lysosomal degradation process for cytoplasmic constituents that occurs during stress conditions. To

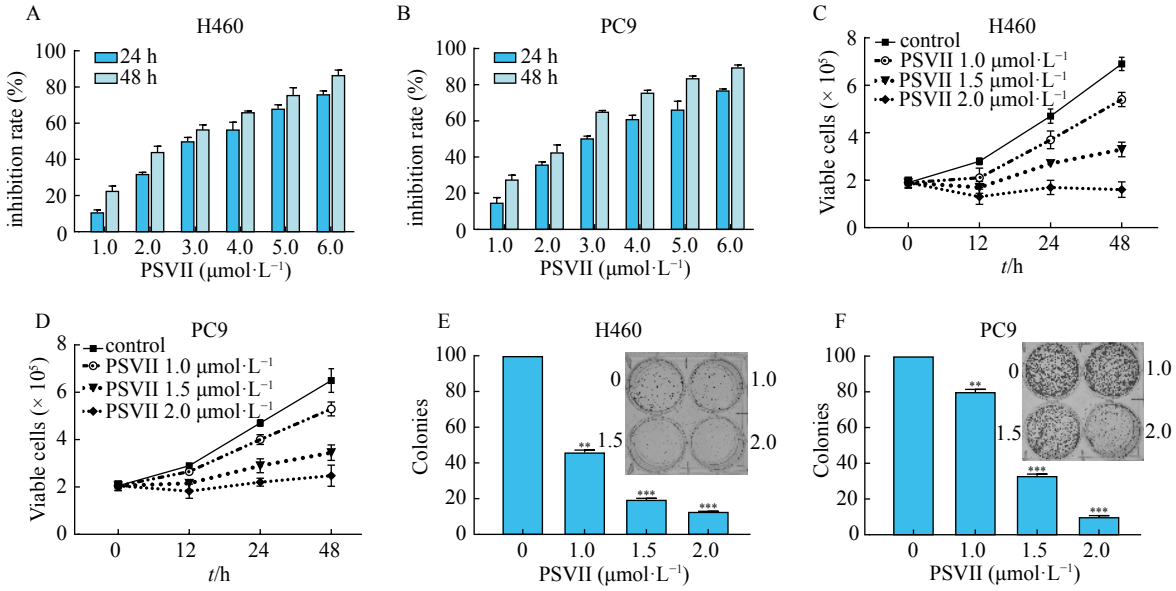

Fig. 2 Effect of PSVII on NSCLC cells. (A–B): Inhibitory effects of PSVII on H460 and PC9 cells were analyzed by CCK-8 assay. (C–D): Inhibitory effects of PSVII on the viability of H460 and PC9 cells were assayed by trypan blue exclusion assay. (E–F): Colony formation assays of H460 and PC9 cells treated with PSVII at the indicated concentrations. The data are representative of at least three experiments. $^{*}P < 0.05$, $^{**}P < 0.01$, $^{***}P < 0.001$ *vs* control

Table 1 IC_{50} values of PSVII on NSCLC cell lines

Cell lines	16-HBE	A549	H1299	NCI-H820	H460	PC9
IC_{50} (μmol·L^{-1})	7.62 ± 0.51	5.59 ± 0.08	4.37 ± 0.48	3.52 ± 0.67	3.16 ± 0.23	2.86 ± 0.26

The cells were treated with PSVII at various concentrations for 24 h, the cell cytotoxicity was analyzed by CCK-8 assay, and the IC_{50} was calculated using CalcuSyn (version 2.1). Values shown are means plus or minus SD of quadruplicate determinations.

detect whether PSVII induces the formation of autophagosomes, an exogenous GFP-LC3 plasmid was transfected into H460 and PC9 cells, which were then treated with PSVII for 24 h, followed by confocal microscopy assessment. We showed that while control cells displayed diffuse staining, upon PSVII treatment, H460 (Fig. 4A) and PC9 (Fig. 4B) cells exhibited a speckled fluorescent staining pattern, indicating the redistribution of LC3 to autophagosomes. Next, to investigate the relationship between PSVII and autophagy, we tested the expression levels of the lipidated form of LC3 (LC3II) and p62, which are specific markers of autophagy [27-28]. The results showed that the expression levels of LC3II and p62 in PSVII-treated H460 and PC9 cells were significantly increased (Fig. 4C), indicating that PSVII treatment induces autophagy. We hypothesized that the cytotoxicity of PSVII is related to autophagy induction and the autophagic death of NSCLC cells. PSVII and the autophagy inhibitor 3-MA were combined and used to treat NSCLC cells (Fig. 4D). Furthermore, we showed that 3-MA significantly reversed the cell proliferation that was inhibited by PSVII (Fig. 4E) and the cell apoptosis that was induced by PSVII (Fig. 4F). These results suggested that PSVII may induce apoptosis of NSCLC cells by activating autophagy. In addition to initiating autophagy, our previous experimental results also showed that PSVII significantly increased the expression of p62 in NSCLC cells, which is the substrate of autophagy and is transported to lysosomes for degradation, suggesting that autophagic flux may be blocked. Furthermore, exogenous mCherry-EGFP-LC3 was transfected into the cells (Fig. 4G). The results showed that the yellow fluorescence increased significantly after PSVII treatment, suggesting the fusion of autophagosomes was blocked. The lysosome was impaired, and autophagic flux was blocked.

PSVII induces autophagy via AMPK activation in NSCLC cells

AMPK/mTOR signaling is the main autophagy regulatory pathway. The expression of AMPK and its downstream mTOR signaling was detected by western blot. As shown in Fig. 5A, we confirmed that the phosphorylation of AMPKα at THR-172 (pAMPKα) was upregulated in H460 and PC9 cells following treatment with PSVII for 24 h. Further investigation of the mTOR signaling pathway showed that PSVII downregulated the phosphorylation of mTOR at SER-2448 (Fig. 5B). This downregulation subsequently repressed the phosphorylation of key proteins involved in transcription, such as eukaryotic initiation factor 4E binding protein 1 (4EBP1) at THR-37/46, and P70S6 kinase (P70S6K) at THR-389 in a dose-dependent manner without affecting the levels of total mTOR, 4EBP1, and P70S6K, leading to the repression of mTORC1 activity. To further investigate the role of

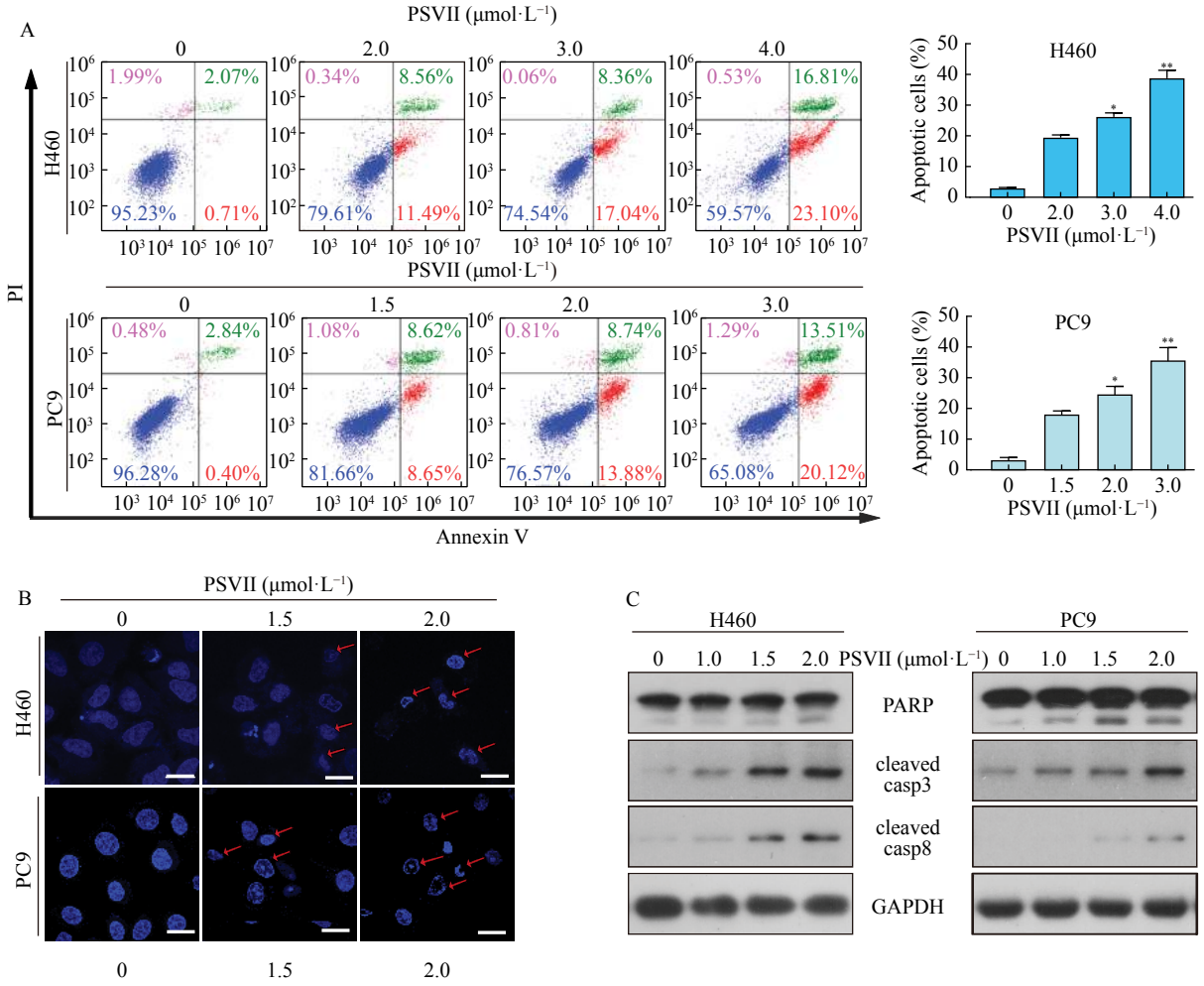

Fig. 3 PSVII induces apoptosis in NSCLC cells. (A): H460 or PC9 cells were treated with PSVII for 24 h, and cell apoptosis was assessed by annexin V/PI staining and flow cytometry. (B): H460 or PC9 cells were incubated with various doses of PSVII for 24 h. The cells were examined by DAPI staining. Scale bar = 20 μm. (C): H460 or PC9 cells were treated with increasing concentrations of PSVII for 24 h. Western blot was performed using the indicated antibodies. GAPDH was used as the loading control. The data are representative of at least three experiments. $^{*}P < 0.05$, $^{**}P < 0.01$, $^{***}P < 0.001$ *vs* control

AMPK in PSVII-induced autophagy in NSCLC cells, compound C (CC), a specific AMPK inhibitor, was used to inactivate AMPK [29]. As shown in Figs. 5C–5E, CC downregulated the PSVII-induced upregulation of pAMPKα and decreased the PSVII-induced accumulation of LC3II. In addition, we found that after CC blocked AMPK signal, PSVII's proliferation inhibition and apoptosis induction were also significantly inhibited (Figs. 5F–5H). In summary, these results suggest that PSVII induces autophagy and apoptosis by activating AMPK in NSCLC cells.

PSVII is a direct activator of AMPK

Next, we determined whether PSVII modulates AMPK kinase activity. For this purpose, H460 and PC9 cells were treated with PSVII and incubated for different times (12 and 24 h). The AMPK activity assay revealed a significant increase in AMPK activity after PSVII treatment in the two cell lines (Figs. 6A–6B). These results confirmed that PSVII is a potent AMPK activator.

We further determined the interaction of PSVII and AMPK *in silico*. Molecular docking experiments were conducted between PSVII and the crystal structure of AMPK (PDB code: 4CFF) by using AutoDock 4. Among the α, β, and γ subunits, there was an ADaM site (allosteric drug and metabolite site), which was constructed by the catalytic kinase domain of the α subunit and the regulatory carbohydrate-binding module (CBM) of the β subunit. PSVII bound to the ADaM site with a binding energy of –4. 51 Kcal/mol (Fig. 6C) and interacted with a cluster of hydrophobic residues from each domain: ASP-20$_{(Kinase)}$, THR-21$_{(Kinase)}$, GLY-23$_{(Kinase)}$, VAL-24$_{(Kinase)}$, LYS-29$_{(Kinase)}$, ASN-48$_{(Kinase)}$, LYS-51$_{(Kinase)}$, ARG-83$_{(CBM)}$, and HIS-109$_{(CBM)}$ (Fig. 6D). It is important to note that the hydroxyl groups on PSVII formed hydrogen bonds with ASP-20, GLY-23, and VAL-24; the bond lengths of the hydrogen bonds were 2.8 Å, 2.7 Å, and 2.0 Å, respectively. Next, we employed microscale thermophoresis (MST) and drug affinity responsive targeting sta-

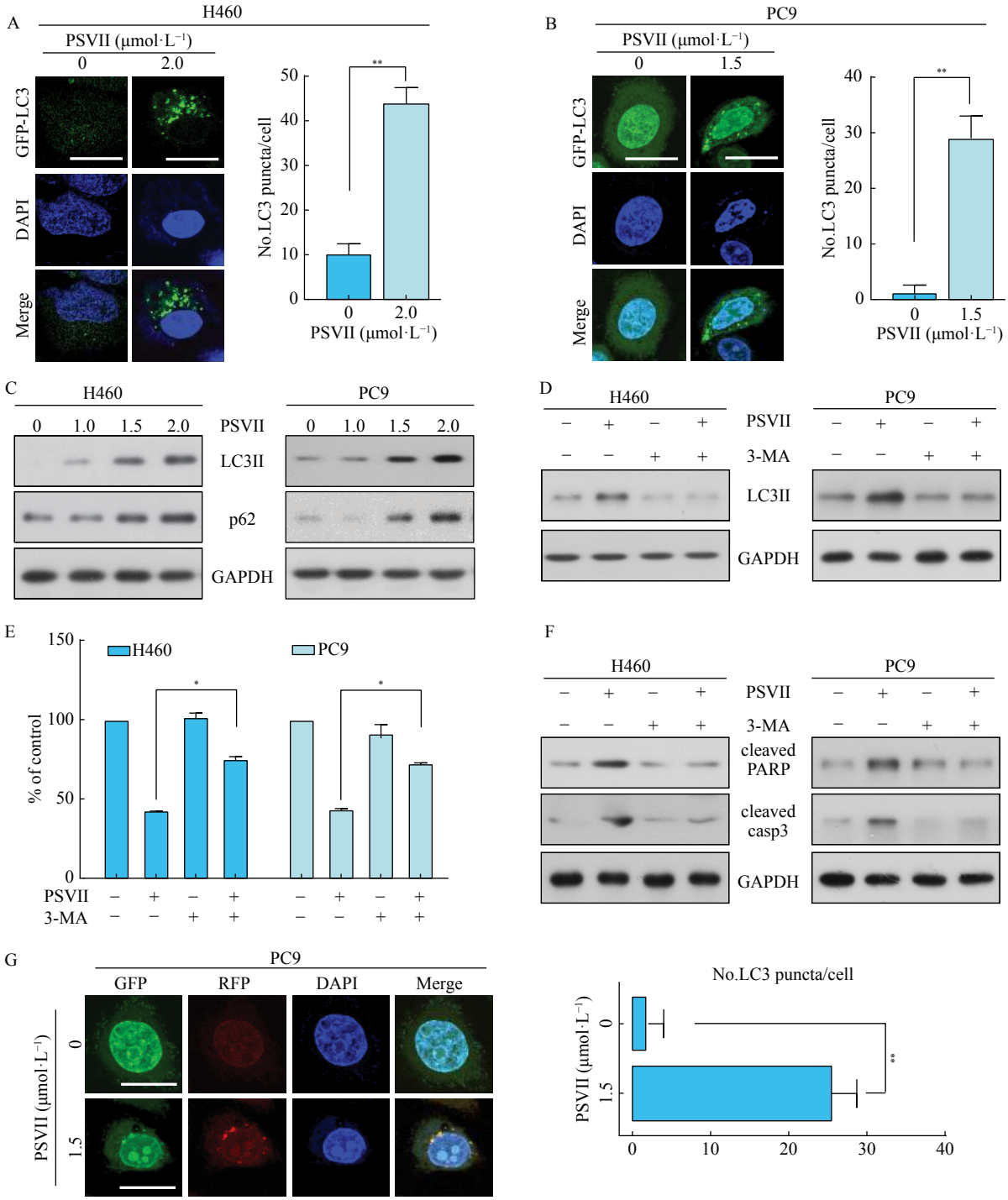

Fig. 4 PSVII induces autophagy in NSCLC cells. (A–B): H460 or PC9 cells transfected with the pQCXIP-GFP-LC3 plasmid were treated with PSVII for 24 h and assessed by immunofluorescence analyses. Scale bar = 20 μm. The graph shows the quantification of LC3II-positive puncta in cells. (C): H460 or PC9 cells were treated with increasing concentrations of PSVII for 24 h. Western blot was performed using the indicated antibodies. (D): H460 or PC9 cells were treated with PSVII (1.5 μmol·L^{-1}) and/or 3-MA (1 mmol·L^{-1}) for 24 h and analyzed by Western blot. (E): H460 or PC9 cells were treated with PSVII (1.5 μmol·L^{-1}) and/or 3-MA (1 mmol·L^{-1}) for 24 h and analyzed by CCK-8 assay. (F): H460 or PC9 cells were treated with PSVII (1.5 μmol·L^{-1}) and/or 3-MA (1 mmol·L^{-1}) for 24 h and analyzed by Western blot. (G): PC9 cells were transfected with mCherry-GFP-LC3 for 24 h and treated with PSVII for another 24 h. Autophagic flux was examined. Scale bar = 15 μm

bility (DARTS) assays to further detect the PSVII/AMPK interaction. For MST, we detected that the equilibrium dissociation constant (K_d) value of PSVII and AMPK was measured and elucidated as 10.52 ± 1.17 nmol·L^{-1}, and the signal to noise is 44.5, which indicated a relatively strong binding affinity (Fig. 6E). Furthermore, the DARTS assay relies on the

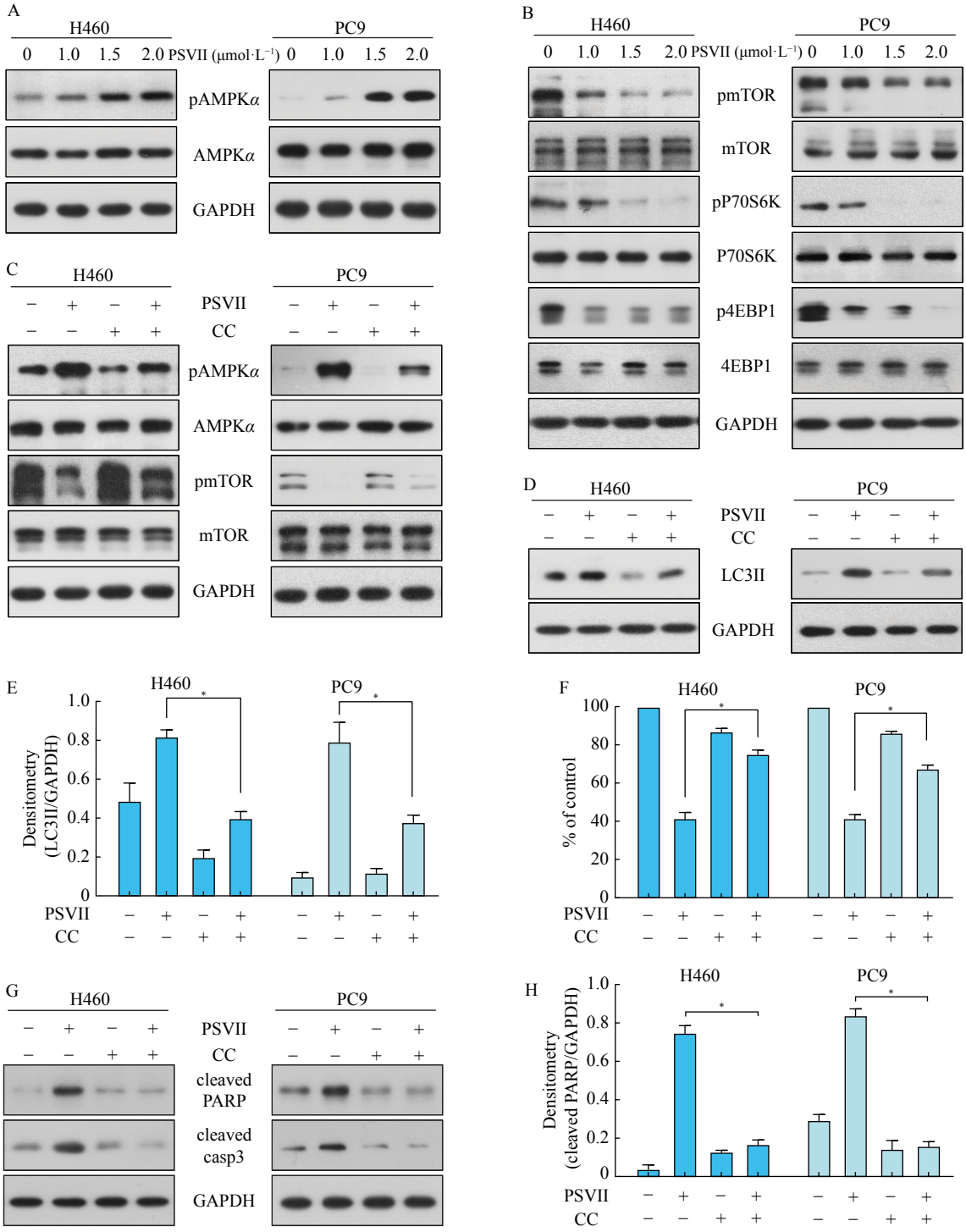

Fig. 5 PSVII induces autophagy *via* AMPK activation in NSCLC cells. (A–B): H460 or PC9 cells were treated with increasing concentrations of PSVII for 24 h. Western blot was performed using the indicated antibodies. (C–D): H460 or PC9 cells were treated with PSVII (1.5 μmol·L^{-1}) and/or compound C (CC, 30 μmol·L^{-1}) for 24 h, and Western blot was performed using the indicated antibodies. (E): Densitometric analyses of LC3II/GAPDH in (D). (F): H460 or PC9 cells were treated with PSVII (1.5 μmol·L^{-1}) and/or compound C (CC, 30 μmol·L^{-1}) for 24 h, and CCK-8 assay was performed to detect proliferation. (G): H460 or PC9 cells were treated with PSVII (1.5 μmol·L^{-1}) and/or compound C (CC, 30 μmol·L^{-1}) for 24 h, and Western blot was performed using the indicated antibodies. (H): Densitometric analyses of cleaved PARP/GAPDH in (G). The data are representative of at least three experiments.

idea that drug-target engagement protects against proteolysis of the target protein. As shown in Fig. 6F, PSVII significantly prevented the pronase-induced proteolysis of AMPK. Conclusively, these results demonstrated that PSVII directly

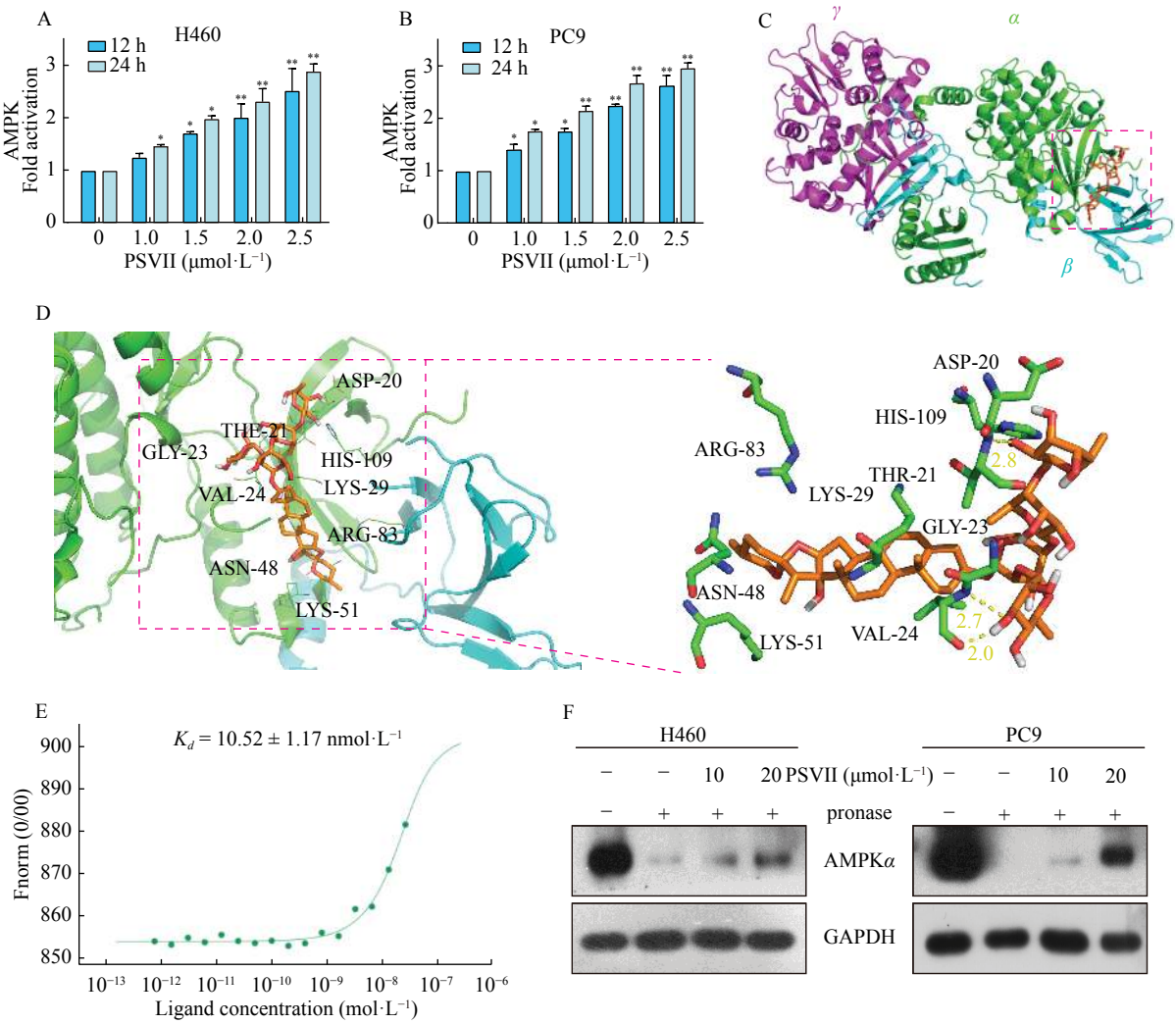

Fig. 6 PSVII is a direct activator of AMPK. (A–B): H460 or PC9 cells were treated with increasing concentrations of PSVII for 24 h, and an AMPK activity assay was performed. (C): The binding mode of PSVII docked to AMPK. (D): The binding mode of PSVII docked to AMPK. The *α* subunit is green, the *β* subunit is cyan, the *γ* subunit is magenta and PSVII is gold. The main residues involved in drug interactions are shown as labeled green sticks. (E): Binding affinity of PSVII with AMPK by MST in standard treated capillaries. (E): Cell lysates were incubated in the presence or absence of PSVII for 30 min at room temperature, followed by proteolysis with pronase. GAPDH, which served as the loading control, is relatively resistant to proteolysis. $^{*}P < 0.05$, $^{**}P < 0.01$ *vs* control. The data are representative of at least three experiments.

binds with AMPK.

Discussion

PSVII induces apoptosis in several human cancer cell lines, such as adriamycin-resistant human chronic myeloid leukemia cells (K562/ADR) [17]; and human colorectal cancer HT-29 and HCT-116 cells [30], and induces autophagy in NSCLC A549 cells [31]. However, the molecular target has not been clearly determined. Here, we demonstrated that PSVII induces not only apoptosis but also autophagy in NSCLC cells by directly activating AMPK. We explored the effects of PSVII on the NSCLC cell lines H460 and PC9, and found that PSVII exhibited cytotoxic effects on NSCLC cells in both concentration- and time-dependent manners (Fig. 2).

Autophagy plays a dual role in tumorigenesis, which has been confirmed by extensive research: autophagy suppresses the early growth of tumors, but it is involved in promoting late or invasive tumors [32-33]. Today, autophagy has become a new type of anticancer target. Several natural compounds with anticancer effects have been found to induce autophagy in cancer cells. Here, we confirmed the effect of PSVII on autophagy induction in NSCLC cells. Importantly, treatment with the autophagy inhibitor 3-MA blocked PSVII-inhibited proliferation and PSVII-induced apoptosis in NSCLC cells, suggesting that activation of autophagy in NSCLC cells contributes to the anticancer effect of PSVII. Interestingly, we found that the suppression of autophagy leads to the inhibition of apoptosis, which indicates that the occurrence of apoptosis is caused by autophagy. Both autophagy and apoptosis are involved in the occurrence and development of tumor

cells, but their specific regulatory mechanisms and interrelationships need further study to provide useful clues for tumor prevention and treatment. Furthermore, we demonstrate that PSVII inhibited autophagic flux (Fig. 4). Disturbed autophagic flux in different tissues and cells often hampers the removal of pathogenic proteins and damaged organelles, which may cause cells to become sensitive to death [34]. Based on these findings, we propose that PSVII-mediated inhibition of proliferation and activation of apoptosis in NSCLC cells may be partially attributed to autophagy activation and autophagic flux inhibition.

It is well known that autophagy is regulated by a complex network. Among them, the AMPK/mTORC1 pathway has been well characterized. Autophagy is positively enhanced by AMPK activation and negatively regulated by mTOR activation [35-37]. It was discovered that autophagy associated with AMPK/mTORC1 plays a crucial role in cancer treatment [38]. Here, we found that PSVII increased the phosphorylation of AMPK in NSCLC cell lines and reduced the activation of mTORC1. To further demonstrate this, we used an AMPK inhibitor (compound C) to evaluate its effect on PSVII-induced autophagy. As expected, compound C reversed the PSVII-induced upregulation of pAMPK and significantly inhibited the PSVII-induced proliferation inhibition, autophagy, and apoptosis (Fig. 5). These results illustrate that the AMPK/mTOR pathway plays a crucial role in PSVII-induced autophagy activation and anticancer effects.

In silico modeling indicated that the ADaM active site of AMPK was the preferred binding site for PSVII (Fig. 6C). Several direct AMPK activators (A-769662 [39], salicylate [40] and compound 991 [41]) were directly targeted to bind to the ADaM active site and showed better potency. These activators either directly activate AMPKα by enhancing protection against THR-172 dephosphorylation or indirectly activate AMPKα by maintaining the conformation of the β subunit. PSVII interacted with a cluster of hydrophobic residues ASP-$20_{(Kinase)}$, THR-$21_{(Kinase)}$, GLY-$23_{(Kinase)}$, VAL-$24_{(Kinase)}$, LYS-$29_{(Kinase)}$, ASN-$48_{(Kinase)}$, LYS-$51_{(Kinase)}$, ARG-$83_{(CBM)}$, and HIS-$109_{(CBM)}$ (Fig. 6D). It is important to note that the hydroxyl groups on PSVII formed three hydrogen bonds with ASP-20, GLY-23, and VAL-24, with bond lengths of 2.8 Å, 2.7 Å, and 2.0 Å, respectively, suggesting that PSVII and ADaM active sites form a relatively stable binding relationship. Moreover, from the amino acid residues bound to PSVII, it can be seen that most of the residues are located in the kinase region of the AMPKα subunit, and three of them can form hydrogen bonds with PSVII. These results indicate that PSVII directly activates AMPKα by enhancing protection against THR-172 dephosphorylation. Phosphorylation of THR-172 is then maintained to maintain AMPK activity. MST and DARTS, are novel methods to detect direct drug-target interactions. We applied these methods to confirm the interaction between PSVII and AMPK inside and outside of the cells (Figs. 6E and 6F), which indicated that PSVII directly binds to AMPK.

In summary, this study has provided a natural compound, PSVII, which directly binds to the ADaM site of AMPK and activates AMPK, exhibiting an anticancer effect on NSCLC cells. PSVII activates autophagy through AMPK/mTOR signaling to inhibit cancer cell proliferation. Our findings suggest that PSVII is a potential agent for treating NSCLC and a promising drug for AMPK activator research.

References

[1] Siegel RL, Miller KD, Jemal A. Cancer statistics, 2018 [J]. *CA Cancer J Clin*, 2018, **68**(1): 7-30.

[2] Chen W, Zheng R, Baade PD, *et al*. Cancer statistics in China, 2015 [J]. *CA Cancer J Clin*, 2016, **66**(2): 115-132.

[3] Siegel RL, Miller KD, Jemal A. Cancer statistics, 2016 [J]. *CA Cancer J Clin*, 2016, **66**(1): 7-30.

[4] Miller KD, Siegel RL, Lin CC, *et al*. Cancer treatment and survivorship statistics, 2016 [J]. *CA Cancer J Clin*, 2016, **66**(4): 271-289.

[5] Wald O. CXCR4 based therapeutics for non-small cell lung cancer (NSCLC) [J]. *J Clin Med*, 2018, **7**(10): 303.

[6] Rubinsztein DC, Marino G, Kroemer G. Autophagy and aging [J]. *Cell*, 2011, **146**(5): 682-695.

[7] Limpert AS, Lambert LJ, Bakas NA, *et al*. Autophagy in cancer: Regulation by small molecules [J]. *Trends Pharmacol Sci*, 2018, **39**(12): 1021-1032.

[8] Doherty J, Baehrecke EH. Life, death and autophagy [J]. *Nat Cell Biol*, 2018, **20**(10): 1110-1117.

[9] Liu EY, Ryan KM. Autophagy and cancer--issues we need to digest [J]. *J Cell Sci*, 2012, **125**(Pt 10): 2349-2358.

[10] Dyczynski M, Yu Y, Otrocka M, *et al*. Targeting autophagy by small molecule inhibitors of vacuolar protein sorting 34 (Vps34) improves the sensitivity of breast cancer cells to Sunitinib [J]. *Cancer Lett*, 2018, **435**: 32-43.

[11] Hardie DG, Ross FA, Hawley SA. AMPK: a nutrient and energy sensor that maintains energy homeostasis [J]. *Nat Rev Mol Cell Biol*, 2012, **13**(4): 251-262.

[12] Han F, Li CF, Cai Z, *et al*. The critical role of AMPK in driving Akt activation under stress, tumorigenesis and drug resistance [J]. *Nat Commun*, 2018, **9**(1): 4728.

[13] De Veirman K, Menu E, Maes K, *et al*. Myeloid-derived suppressor cells induce multiple myeloma cell survival by activating the AMPK pathway [J]. *Cancer Lett*, 2019, **442**: 233-241.

[14] Zhang YF, Huang P, Liu XW, *et al*. Polyphyllin I inhibits growth and invasion of cisplatin-resistant gastric cancer cells by partially inhibiting CIP2A/PP2A/Akt signaling axis [J]. *J Pharmacol Sci*, 2018, **137**(3): 305-312.

[15] Wang BL, Zhang H, Hao XC, *et al*. Research progress on pharmacological action of trillium tschonoskii Maxim [J]. *Int J Tradit Chin Med*, 2018, **40**(5): 478-481.

[16] Wang BL, Hao XC, Ge ZK, *et al*. Study on HPLC fingerprint of *Trillium tschonoskii* Maxim [J]. *J Hubei Univ Med*, 2018, **37**(3): 225-228.

[17] Yan T, Hu GS, Wang AH, *et al*. Paris saponin VII induces cell cycle arrest and apoptosis by regulating Akt/MAPK pathway and inhibition of P-glycoprotein in K562/ADR cells [J]. *Phytother Res*, 2018, **32**(5): 898-907.

[18] Li YH, Sun Y, Fan L, *et al*. Paris saponin VII inhibits growth of colorectal cancer cells through Ras signaling pathway [J]. *Biochem Pharmacol*, 2014, **88**(2): 150-157.

[19] Zhang WJ, Zhang D, Ma X, *et al*. Paris saponin VII suppressed the growth of human cervical cancer Hela cells [J]. *Eur J Med Res*, 2014, **19**: 41.

[20] Fan L, Li YH, Sun Y, *et al*. Paris saponin VII inhibits the migration and invasion in human A549 lung cancer cells [J].

Phytother Res, 2015, **29**(9): 1366-1372.
[21] Cheng G, Gao FG, Sun XJ, *et al*. Paris saponin VII suppresses osteosarcoma cell migration and invasion by inhibiting MMP2/9 production *via* the p38 MAPK signaling pathway [J]. *Mol Med Rep*, 2016, **14**(4): 3199-3205.
[22] Ma WJ, Xiang YC, Yang R, *et al*. Cucurbitacin B induces inhibitory effects *via* the CIP2A/PP2A/C-KIT signaling axis in t(8;21) acute myeloid leukemia [J]. *J Pharmacol Sci*, 2019, **139**(4): 304-310.
[23] Liu PF, Xiang YC, Liu XW, *et al*. Cucurbitacin B induces the lysosomal degradation of EGFR and suppresses the CIP2A/PP2A/Akt signaling axis in gefitinib-resistant non-small cell lung cancer [J]. *Molecules*, 2019, **24**(3): 647.
[24] Si Y, Wang J, Liu XW, *et al*. Ethoxysanguinarine, a novel direct activator of AMP-activated protein kinase, induces autophagy and exhibits therapeutic potential in breast cancer cells [J]. *Front Pharmacol*, 2019, **10**: 1503.
[25] Wang QW, Zhang QA, Luan SS, *et al*. Adapalene inhibits ovarian cancer ES-2 cells growth by targeting glutamic-oxaloacetic transaminase 1 [J]. *Bioorg Chem*, 2019, **93**: 103315.
[26] Choi J, Lee YJ, Yoon YJ, *et al*. Pimozide suppresses cancer cell migration and tumor metastasis through binding to ARPC2, a subunit of the Arp2/3 complex [J]. *Cancer Sci*, 2019, **110**(12): 3788-3801.
[27] Lee YK, Jun YW, Choi HE, *et al*. Development of LC3/GABARAP sensors containing a LIR and a hydrophobic domain to monitor autophagy [J]. *Embo J*, 2017, **36**(8): 1100-1116.
[28] Bjorkoy G, Lamark T, Pankiv S, *et al*. Monitoring autophagic degradation of p62/SQSTM1 [J]. *Methods Enzymol*, 2009, **452**: 181-197.
[29] Shen QW, Gerrard DE, Du M. Compound C, an inhibitor of AMP-activated protein kinase, inhibits glycolysis in mouse longissimus dorsi postmortem [J]. *Meat Sci*, 2008, **78**(3): 323-330.
[30] Zhou HP, Sun Y, Zheng HN, *et al*. Paris saponin VII extracted from trillium tschonoskii suppresses proliferation and induces apoptosis of human colorectal cancer cells [J]. *J Ethnopharmacol*, 2019, **239**: 111903.
[31] Qian S, Tong S, Wu J, *et al*. Paris saponin VII extracted from *Trillium tschonoskii* induces autophagy and apoptosis in NSCLC cells [J]. *J Ethnopharmacol*, 2020, **248**: 112304.
[32] Denton D, Kumar S. Autophagy-dependent cell death [J]. *Cell Death Differ*, 2019, **26**(4): 605-616.
[33] Kriel J, Loos B. The good, the bad and the autophagosome: exploring unanswered questions of autophagy-dependent cell death [J]. *Cell Death Differ*, 2019, **26**(4): 640-652.
[34] Hua F, Li K, Yu JJ, *et al*. TRB3 links insulin/IGF to tumour promotion by interacting with p62 and impeding autophagic/proteasomal degradations [J]. *Nat Commun*, 2015, **6**: 7951.
[35] Tavakol S, Ashrafizadeh M, Deng S, *et al*. Autophagy modulators: Mechanistic aspects and drug delivery systems [J]. *Biomolecules*, 2019, **9**(10): 530.
[36] Zhou YY, Li Y, Jiang WQ, *et al*. MAPK/JNK signalling: a potential autophagy regulation pathway [J]. *Biosci Rep*, 2015, **35**(3): e00199.
[37] Sui XB, Kong N, Ye L, *et al*. p38 and JNK MAPK pathways control the balance of apoptosis and autophagy in response to chemotherapeutic agents [J]. *Cancer Lett*, 2014, **344**(2): 174-179.
[38] Sohretoglu D, Zhang C, Luo J, *et al*. ReishiMax inhibits mTORC1/2 by activating AMPK and inhibiting IGFR/PI3K/Rheb in tumor cells [J]. *Signal Transduct Target Ther*, 2019, **4**: 21.
[39] Shin DH, Choi YJ, Park JW. SIRT1 and AMPK mediate hypoxia-induced resistance of non-small cell lung cancers to cisplatin and doxorubicin [J]. *Cancer Res*, 2014, **74**(1): 298-308.
[40] Liao CR, Kuo YH, Ho YL, *et al*. Studies on cytotoxic constituents from the leaves of *Elaeagnus oldhamii* Maxim. in non-small cell lung cancer A549 cells [J]. *Molecules*, 2014, **19**(7): 9515-9534.
[41] Bultot L, Jensen TE, Lai YC, *et al*. Benzimidazole derivative small-molecule 991 enhances AMPK activity and glucose uptake induced by AICAR or contraction in skeletal muscle [J]. *Am J Physiol Endocrinol Metab*, 2016, **311**(4): E706-E719.

Cite this article as: XIANG Yu-Chen, SHEN Jie, SI Yuan, LIU Xue-Wen, ZHANG Liang, WEN Jun, ZHANG Te, YU Qing-Qing, LU Jun-Fei, XIANG Ke, LIU Ying. Paris saponin VII, a direct activator of AMPK, induces autophagy and exhibits therapeutic potential in non-small-cell lung cancer [J]. *Chin J Nat Med*, 2021, **19**(3): 195-204.